ChemSusChem

Research Article
doi.org/10.1002/cssc.202401813

Chemistry Europe
European Chemical Societies Publishing

www.chemsuschem.org

Amino Acid-Based Ionic Liquids-Aided CO_2 Hydrogenation to Methanol

Ayeshe Moazezbarabadi,[a] Anja Kammer,[a] Elisabetta Alberico,*[a, b] Henrik Junge,*[a] and Matthias Beller*[a]

This study explored the use of amino acid-based ionic liquids to facilitate the conversion of carbon dioxide (CO_2) into methanol through catalytic hydrogenation. Combining tetrabutylammonium L-argininate (TBA·Arg) with the ruthenium Ru-MACHO-BH complex allowed achieving significant yields of methanol under optimized conditions, with a turnover number (TON) up to 700. By systematically varying key reaction parameters, we demonstrated that the TBA·Arg ionic liquid promotes the efficient hydrogenation pathway leading to methanol formation, thus offering a sustainable approach to CO_2 valorization. These findings underscore the potential of amino acid-based ionic liquids in catalyzing the transformation of CO_2 into valuable chemicals, contributing to carbon mitigation efforts.

Introduction

The increasing concentration of carbon dioxide in the atmosphere due to human activities in the past 150 years is leading to global climate change and many environmental concerns. Each year we are experiencing a new record high CO_2 concentration and in 2023 the peak value reached 19.3 parts per million, 50 percent higher than it was before the Industrial Revolution.[1] In the 2015 Paris climate agreement (COP21), representatives of more than 190 countries pledged to limit global warming to within 1.5 °C of pre-industrial levels.[2]

In the transition to the adoption of sustainable alternatives which ultimately stop the production and use of fossil fuels, efforts are being devoted to reduce unavoidable emissions so as to achieve net zero by 2050.[4,5] In this respect, technologies for the capture of carbon dioxide, also from dilute sources, such as flue gases and air, and its storage are being developed and deployed to contribute carbon mitigation.[6] To advantageously exploit captured CO_2, as a C1 feedstock,[8] and reduce the energy and capital costs required for CO_2 desorption and compression, the integration of capture and conversion is however preferable. To this goal, processes are being designed in which the direct transformation of the captured and "reactive" CO_2 affords valuable products while regenerating the capturing agent.[9] In this context, the catalytic hydrogenation of captured CO_2,[12] preferentially with green hydrogen obtained through water splitting using renewable energy, represents an alternative route to methanol which does not rely on the use of fossil fuel-derived syn gas.[17]

Methanol is an important organic feedstock in the chemical industry which is produced annually on the 100 Mt scale, more than 60% of which is used to synthesize chemicals such as formaldehyde, acetic acid, methyl methacrylate, and ethylene and propylene through the methanol-to-olefin (MTO) route.[19] Methanol can also be used as a fuel, either by itself, in a blend with gasoline, for the production of biodiesel, or in the form of methyl tert-butyl ether (MTBE) and dimethyl ether (DME).

In the past decade, several homogeneous catalytic systems, mainly employing ruthenium complexes, have been developed which, while still far away from practical application, allow for the hydrogenation of CO_2 to CH_3OH under relatively mild conditions.[15–16] They can be classified in two broad categories, depending on whether they operate in a neutral/slightly acidic medium or in a basic one. In the former case, HCOOH, formed by initial reduction of CO_2, is converted into a formic acid ester, the hydrogenation of which, affords CH_3OH. Base-compatible catalysts instead should be better-suited for hydrogenation of CO_2 in solutions including amines. The latter systems might be advantageous because chemical absorption into aqueous solutions of monoethanolamine (MEA), diethanolamine (DEA), and methyldiethanolamine (MDEA) represents the current commercial technology for CO_2 capture from flue gases.[22]

The first proof of concept describing the domino use of a secondary amine which could serve as capturing agent for CO_2 and a catalyst Ru-MACHO-BH **Ru-1** for the hydrogenation of the resulting carbamate to methanol via formamide (Scheme 1) was published by Sanford in 2015.[23] In a water-lean organic solvent, CO_2 is first chemisorbed through reaction with the amine in a 1:2 ratio to afford an ammonium carbamate. **Ru-1** then catalyzes its hydrogenation to ammonium formate, which is thermally dehydrated to formamide. **Ru-1** eventually promotes

[a] *Leibniz-Institut für Katalyse e.V. an der Universität Rostock, Rostock, Germany*
[b] *Istituto di Chimica Biomolecolare – CNR, Sassari, Italy*

Correspondence: *Elisabetta Alberico, Henrik Junge and Matthias Beller, Leibniz-Institut für Katalyse e.V. an der Universität Rostock, Albert-Einstein-Str. 29a, 18059 Rostock, Germany.*
Email: elisabetta.alberico@cnr.it and henrik.junge@catalysis.de and matthias.beller@catalysis.de

Supporting information for this article is available on the WWW under https://doi.org/10.1002/cssc.202401813

a. Methanol synthesis through **Ru-1**-promoted **hydrogenation** of CO_2

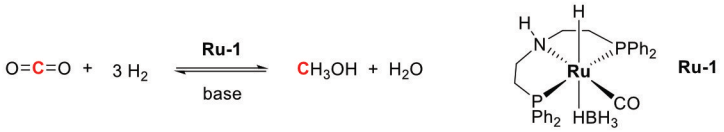

b. Methanol synthesis through CO_2 amine-promoted **capture** and **Ru-1**-promoted **hydrogenation**

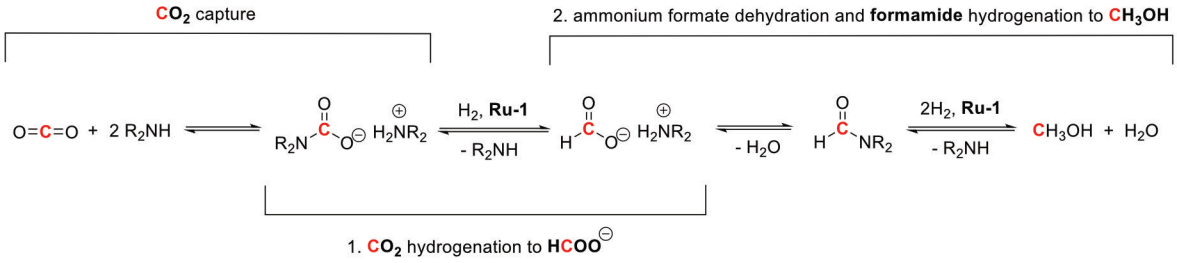

c. Selected examples of CO_2 amine-promoted **capture** and **Ru-1**-promoted **hydrogenation** to methanol

Amine	Conditions		TON_{MeOH}	
Me_2NH	Me_2NH	7.8 mmol	550	Sanford and co., 2015[11]
	K_3PO_4	0.25 mmol		Proof of principle
	Ru-1	1.7 μmol		One-pot step-wise procedure
	THF	2 mL		Volatile amine
	H_2	50 bars		
	CO_2	2.5 bars		
	1. 95 °C	18 h		
	2. 155°C	36 h		
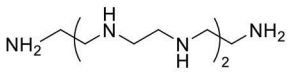 **PEHA** + 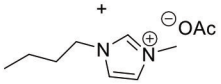 **BMIM·OAc**	PEHA	4.3 mmol	660	Prakash and co., 2024[28]
	BMIM·OAc	1.5 mmol		One-pot
	Ru-1	20 μmol		First report on CO_2 hydrogenation to CH_3OH in IL + polyamine
	Triglyme	5 mL		
	H_2	56.25 bars		
	CO_2	18.75 bars		
	1./ 2. 155 °C	24 h		
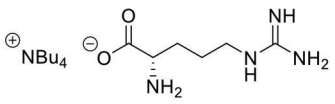 **TBA·Arg**	TBA·Arg	5.0 mmol	700	This work
	Ru-1	2 μmol		One-pot
	THF	10 mL		IL based on amino acid
	H_2	60 bars		Functionalized IL for CO_2 capture
	CO_2	20 bars		
	1./ 2. 150 °C	24 h		

Scheme 1. a. General Equation for **Ru-1**-catalyzed CO_2 hydrogenation to methanol; b. Reactive CO_2 capture: CO_2 capture with amines in water-lean solvents and homogeneous **Ru-1**-catalyzed hydrogenation to formate and methanol; c. Selected examples from the literature showing different approaches for reactive CO_2 capture and hydrogenation to methanol.

hydrogenation of the latter to CH_3OH while regenerating the amine.

Since that first report, several other interesting developments by the groups of Prakash[24] and others[28] have appeared

documenting efforts towards improved solvent (physisorption) and base (chemisorption) CO_2 capturing ability, homogeneous catalyst efficiency, productivity, and selectivity as well as recyclability of the active components. A detailed summary of these works can be found in excellent reviews by Prakash and co-workers.[24, 30] Most of the reported systems rely on the use of amines such as PEHA (pentaethylenehexamine). However, despite their proven efficacy in capturing CO_2, amines are volatile, and undergo thermal- and photo-oxidations which might lead to environmental and health hazards.[31] In this respect, amino acid salt solutions have been proposed as possible alternative by virtue of their lower toxicity and high biodegradability, negligible volatility, but comparable capture performance.[32] More recently, we[34] as well as Leitner and coworkers[36] have demonstrated the possibility to combine the CO_2 capturing ability of the basic amino acids lysine[37] and arginine[38] with the ruthenium[34, 36] and manganese[35] catalyzed homogeneous hydrogenation of CO_2 to generate formates.

Another important issue concerns the nature of the reaction medium: it should warrant a high CO_2 sorption and solubility, be compatible with the hydrogenation conditions, be thermally stable, have very low vapor pressure and allow for easy separation of reaction products. Ionic liquids, which are completely composed of ions and the melting point of which is below 100 °C by definition are promising candidates in this respect and have, therefore, been extensively investigated as CO_2 capturing agents.

Solubility of CO_2 in ionic liquids can be improved by varying the composition and structure of both the cation and anion, although it is primarily affected by the anion.[41] Solubility can be further increased by fluorination and the attachment of long alkyl chains to the cation. Introduction of functional groups, such as amino groups, on either the anion or the cation, can boost their CO_2 sorption capacity through chemisorption. Furthermore, their use as reaction medium, bare or in combination with another solvent, has proved to be beneficial to the catalytic hydrogenation of CO_2 in some cases.[43]

The hydrogenation of CO_2 to formic acid is challenging due to its thermodynamic and kinetic stability.[45] Bases are commonly added to the reaction mixture to shift the thermodynamic equilibrium through the formation of formate salts. Isolation of formic acid is possible through acid addition, though significantly reducing the atom efficiency of the process.

Interestingly, Sans and co-workers have recently reached unprecedented productivity and activity in the catalytic hydrogenation of CO_2 to formic acid without salt formation through the informed design of a ruthenium bis-carbene pyridine CNC-pincer catalyst[46] and the use of 1,2-dimethyl-3-butylimidazolium acetate (BMMI·OAc).[46–47] In combination with an organic solvent and a controlled amount of water, the basic ionic liquid assists the transformation of CO_2 into bicarbonate. The latter is hydrogenated while buffering the solution: in this way the equilibrium is shifted towards the formation of formic acid while the pH never becomes low enough for the catalytically active ruthenium hydride to be protonated and thus quenched.

Das and Nielsen have demonstrated that the basic ionic liquid 1-ethyl-3-methyl-imidazolium acetate can be used both as neat polar solvent, capable of CO_2 capture, and base to promote catalyst activation and productivity.[49] Here, the acid-base equilibrium between the weekly acidic proton at the cation imidazolium C(2) and the accompanying anion acetate ensures a certain concentration of free carbene which will add to CO_2 activating it for hydrogenation.[50] By combining the ionic liquid with a pincer bisphosphinoamino ruthenium complex, they created a robust, flexible, and stable catalytic system for the co-solvent- and additive-free, reversible hydrogenation of CO_2 to formic acid as well as formic acid dehydrogenation under very mild conditions.[49] None of the examples reported so far, relying on the use of amino acids or ionic liquids, describes the reduction of CO_2 to methanol.

Very recently, Prakash has demonstrated that the combination of the ionic liquid 3-butyl-1-methyl imidazolium acetate (BMIM.OAc) and the polyamine PEHA allows the Ru-MACHO-BH **Ru-1**-catalyzed hydrogenation of CO_2 to methanol (Scheme 1).[52] The yield, productivity and activity achieved are better than those accessible when using either the ionic liquid or the amine alone. Compared to the systems affording formate, higher temperatures, up to 155 °C, and higher total pressure, up to 75 bars, were necessary to promote methanol formation. Interestingly, the authors also explored the combination of the same ionic liquid with the amino acid L-arginine in place of PEHA, but only a relatively low TON of 42.5 was recorded.

In this respect, our group has recently shown, for the first time, the possibility to combine the known CO_2 capturing ability of amino acid-based ionic liquids[53] with the *in-situ* conversion of the captured CO_2 to formate salts.[57] Here, the amino acid is not used as an additive but is a constituent of the ionic liquid, it plays the role of the anion. Among those tested, the anion of the basic amino acids L-lysine (Lys) and L-arginine (Arg), carrying an additional amino functionality in their side chain, showed, in combination with the tetrabutylammonium cation (TBA), the highest CO_2 absorption capacity, 1.80 and 1.96 mmol per mmol of adsorbent, respectively. Under a total pressure of 80 bars (H_2/CO_2 1/3) at 80 °C in an aqueous THF solution, in the presence of 5 mmol of TBA·Arg and 10 μmol of Ru-MACHO-BH **Ru-1** a TON of 959 for formate generation was obtained over 24 hrs. The catalytic solution could be recycled up to 5 consecutive times with an overall TON of 12,741. In the present communication, we demonstrate how the same system consisting of the ionic liquid TBA·Arg and MACHO-BH **Ru-1** could be exploited, through adjustment of reaction conditions, for the hydrogenation of CO_2 to CH_3OH, reaching a TON of 700 (Scheme 1).

Results and Discussion

Influence of Ionic Liquid

To investigate the effect of amino acid-based ionic liquids on the Ru-MACHO-BH **Ru-1** promoted hydrogenation of CO_2 to

CH_3OH, initially 11 ionic liquids consisting of different amino acid anions and ammonium cations were prepared according to the corresponding literature procedures.[58] Then, catalytic hydrogenation of carbon dioxide (CO_2/H_2; 20/60 bar) was performed in the presence of these and selected commercially available ILs (each 5.0 mmol) utilizing Ru-MACHO-BH (10 μmol). In our previous work, we had noticed that the condensation of the amino groups with formate to formamide, the key intermediate to access CH_3OH, was not observed below 90 °C and became substantial at 145 °C.[57] Formamide hydrogenation is deemed the most demanding step *en route* to methanol.[63] Therefore, we decided to start our investigation by applying the highest temperature, 165 °C, accessible with the available autoclaves and yet compatible with catalyst Ru-MACHO-BH **Ru-1**, by virtue of its high chemical and thermal stability.[65]

The initial reactions were carried out under a total pressure of 80 bars (H_2/CO_2 1/3), for 24 hours, in tetrahydrofuran to ensure catalyst solubility. The amounts of generated formate and formamide were determined by ^{1}H NMR spectroscopy, while the formed methanol and methyl formate were determined by GC. In addition, all the reactions were checked for CO formation using GC (Figures S1–S6). It should be mentioned that most of the experiments were at least performed twice, and average values are shown in Table 1.

L-argininate- and L-lysinate-tetrabutylammonium (TBA·Arg and TBA·Lys) were investigated first because of their superior performance, as to other amino acid based ionic liquids, in the capture and hydrogenation of CO_2 to formate catalyzed by **Ru-1**.[57] Indeed, in the presence of 5 mmol TBA·Arg, 2.5 mmol of CH_3OH were formed, together with 0.8 mmol $HCOO^-$ and 2.5 mmol formamide (Table 1, entry 1). No formate or CH_3OH were detected when either TBA·Arg or **Ru-1** or CO_2 were absent (Table S2). In comparison, TBA·Lys (Table 1, entry 2) afforded 0.25 mmol $HCOO^-$ and 5.2 mmol formamide but only 0.14 mmol CH_3OH. When TBA·Lys was used, a lysine fragment in the HRMS spectra of post-reaction solutions could be detected (Figure S7), the mass of which indicates that both the α- and ε-amino groups had been formylated under these conditions. In contrast, with TBA·Arg, only the relevant mono-formylated fragment was detected (Figure S8).

For the latter, the α-amino group as the site of formylation[66] was confirmed through the independent synthesis of N-α-formyl-L-arginine and the corresponding TBA-ionic liquid (S4.1, S4.2).

When N-α-formyl-L-arginine was hydrogenated under the same experimental conditions as reported in Table 1, with no CO_2 present, CH_3OH was detected, indicating that the formamide is indeed an entry to CH_3OH (S4.3). Besides, when the TBA·Arg-aided hydrogenation of CO_2 was carried out in the presence of variable amounts of CH_3OH to favor its condensation to methyl formate, under otherwise identical conditions (Table S3, entries 2 and 3), this did not improve the overall yield of CH_3OH, indicating that ester hydrogenation is not the preferred route to CH_3OH. Other ammonium cations in combination with L-arginine were tested, having different substituents at nitrogen, such as N,N,N-trimethyladamantan-1-ammonium (TMAA·Arg, Table 1, entry 3, CH_3OH 1.4 mmol), tetramethylammonium (TMA·Arg, Table 1, entry 4, CH_3OH 1.3 mmol), benzyltrimethylammonium (BTMA·Arg, Table 1, entry 5, CH_3OH 0.94 mmol), choline (CHO·Arg, Table 1, entry 6, CH_3OH 0.54 mmol) and 6-azonia-spiro[5.5]undecane (ASU·Arg, Table 1, entry 7, 0.23 mmol), the latter as an example of more base-resistant cation[68]: none outperformed TBA·Arg as to CH_3OH amount. Replacement of the TBA cation with the analogue phosphonium one TBP (TBP·Arg; Table 1, entry 8) completely suppressed the formation of CH_3OH, despite the comparable productivity in $HCOO^-$ (4.1 mmol $HCOO^-$ and 2.6 mmol formamide). Only a minor amount of CH_3OH, just 0.13 mmol, was obtained when the 1-butyl-3-methylimidazolium cation was used (BMIM·Arg, Table 1, entry 9). The key role played by the L-arginine anion was clearly shown by the fact that little or no CH_3OH was formed when it was replaced by acetate in TBA·Ac (Table 1, entry 10, 0.26 mmol) or chloride in TBA·Cl (Table 1, entry 11), the latter likely acting as a poison to the catalyst. On the other hand, with L-arginine, either alone (Table 1, entry 12) or in combination with added base K_3PO_4 (Table S4, entry 2) or NBu_3 (Table S4, entry 3), only 0.11 mmol of CH_3OH were formed (Table 1, entry 12), thus showing the synergistic effect of the L-argininate/TBA combination on the formation of CH_3OH. Furthermore, TBA·Nor and TBA·GB were prepared from L-norleucine and 4-guanidinobutyric acid, respectively and used to demonstrate the influence of the amino acid side chain on CO_2 hydrogenation. With TBA·Nor, half the amount of formate and formamide (Table 1, entry 13, 0.26 mmol and 2.8 mmol, respectively) were obtained as to TBA·Lys. This is indirect evidence that both amino groups in TBA·Lys can be formylated. But no CH_3OH was obtained. Once both amino groups are formylated, the reaction medium might not be basic enough to promote formamide hydrogenation,[63] which explains the poor yield in CH_3OH. TBA·GB lacks an amino group and in fact very little formate (0.078 mmol) and no formamide were detected (Table 1, entry 14; Figure S6). Yet the amount of CH_3OH is comparable to that obtained with TBA·Arg thus highlighting the key role of the guanidino group in promoting CH_3OH formation (Figure S6). Based on the above results, TBA·Arg was identified as the IL of choice among those tested and was used in further experiments to explore the influence of other key reaction parameters, such as solvent, temperature, relative CO_2/H_2 pressure and catalyst structure.

Influence of Solvent

To begin with, solvents other than THF were tested (Figure 1 and Table S5), as the solvent can affect both the thermodynamics and the kinetics of hydride transfer from the catalyst to the substrate, CO_2 and formamide.[70] Overall, ethers performed best as solvents for CH_3OH formation, except for cyclopentyl methyl ether, where no CH_3OH was detected. The use of alcohol solvents was deleterious as to selectivity, affording very poor yields of CH_3OH but substantial amounts of CO, likely arising from decarbonylation of the corresponding aldehydes, formed through **Ru-1**-promoted alcohol dehydrogenation.[71] This is particularly evident with ethylene glycol, where up to 5.7 mmol

Table 1. Ru-MACHO-BH promoted hydrogenation of CO_2 in the presence of different ionic liquids.

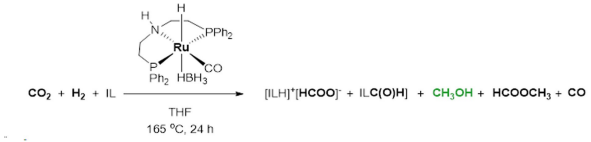

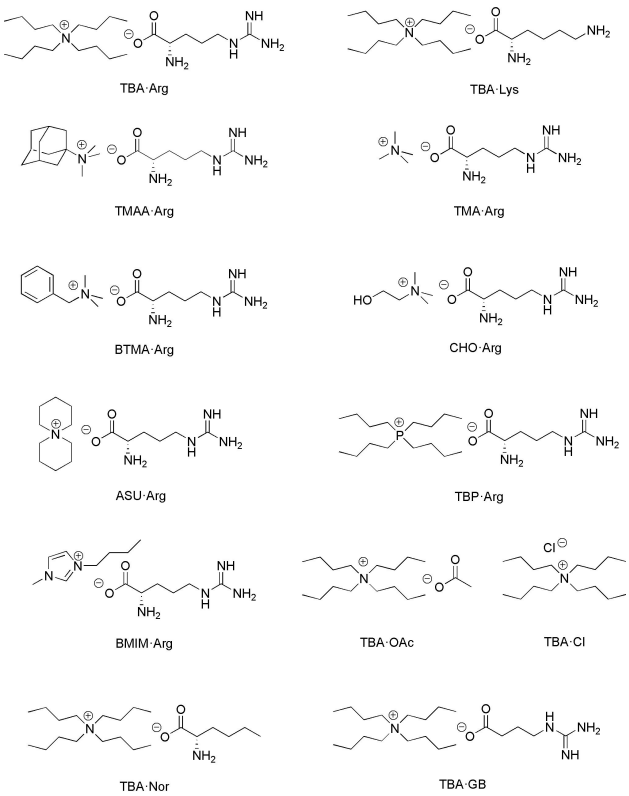

Entry	Ionic liquid	Formate[a] [mmol]	Formamide[a] [mmol]	Methanol[b] [mmol]	methyl formate[b] [mmol]	carbon monoxide[c] [mmol]
1	**TBA·Arg**	0.80	2.5	**2.5**	0.04	0.13
2	**TBA·Lys**	0.25	5.2	**0.14**	n.d.	0.13
3	**TMAA·Arg**	0.76	2.3	**1.4**	0.04	0.04
4	**TMA·Arg**	1.1	2.4	**1.3**	0.06	0.02
5	**BTMA·Arg**	0.98	2.1	**0.94**	0.01	0.02
6	**CHO·Arg**	1.4	1.8	**0.54**	0.01	0.15
7	**ASU·Arg**	3.5	3.8	**0.23**	0.004	0.07
8	**TBP·Arg**	4.1	2.6	**n.d.**	n.d.	0.17
9	**BMIM·Arg**	1.5	2.7	**0.13**	n.d.	0.12
10	**TBA·OAc**	n.d.	n.d.	**0.26**	0.02	0.08
11	**TBA·Cl**	n.d.	n.d.	**n.d.**	n.d.	n.d.
12	**Arg**	1.2	0.83	**0.11**	n.d.	0.06
13	**TBA·Nor**	0.26	2.8	**n.d.**	n.d.	n.d.
14	**TBA·GB**	0.078	n.d.	**2.2**	0.15	0.17

General conditions: Absorbent (5.0 mmol), Ru-MACHO-BH (10 μmol), THF (10 mL), CO_2/H_2 (20/60 bar), 165 °C, 24 h. [a] Determined by ^{1}H NMR with DMF (200 μL, 2.6 mmol) as internal standard. [b] Determined by GC with DMF (200 μL, 2.6 mmol) as internal standard. [c] Determined by gas GC. Experiments in entries 1–6, 9 and 14 were at least performed twice, and average values are shown. Standard deviations of main product amounts (formate, formamide, methanol) are 1–16% of the average (except for formate in entry 4:22% and methyl formate and carbon monoxide amounts $<$0.15 mmol).

of CO were detected (Table S5, entry 10): its facile dehydrogenation to glycolate, despite the high applied H_2 pressure of 70 bars, had been observed also by Prakash in the **Ru-1** catalyzed hydrogenation of CO_2 captured from air with a

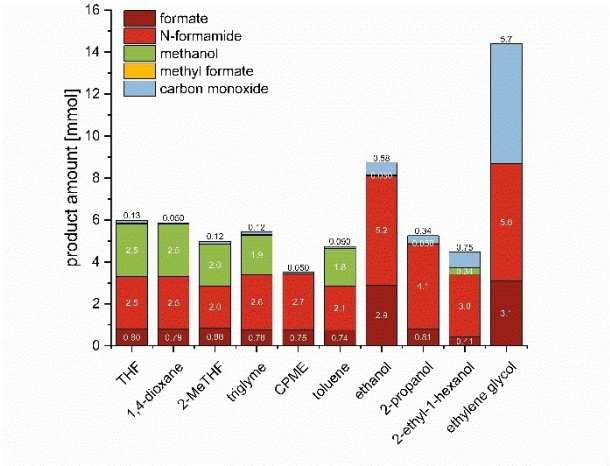

Figure 1. Product distribution as a function of the solvent in the Ru-1 promoted hydrogenation of CO_2. Reaction conditions: TBA·Arg (5.0 mmol), Ru-1 (10 μmol), solvent (10 mL), CO_2/H_2 (20/60 bar), 165 °C, 24 h. CPME = cyclopentyl methyl ether. Numbers represent amounts (mmol) of formate, formamide, methanol, and carbon monoxide, respectively.

solution of hydroxide in ethylene glycol.[26] Because none of the tested other solvents outperformed THF, within error range, the latter was used for further investigations.

Influence of Temperature

Then, the influence of temperature on product yield and distribution, within the range 110–165 °C, was explored (Figure 2 and Table S6). CH_3OH could be detected only above 110 °C, despite the high accumulation of formate (Table S6, entry 1, 11.2 mmol) and formamide (Table S6, entry 1, 4.8 mmol), and its formation, while already observed at 120 °C, became relevant at 150 °C (Table S6, entry 5, 2.0 mmol) and was highest at 165 °C (Table S6, entry 8, 2.5 mmol). This confirms that hydrogenation of formamide to CH_3OH is energetically more demanding than hydrogenation of CO_2 to formate.[63] The latter was almost halved when the temperature was raised from 120–130 °C. In fact, while the absolute amount of formamide only slightly increased from 6.5–6.9 mmol and that of CH_3OH went from 0.03–0.13 mmol, the amount of formate dropped from 8.8 mmol–1.7 mmol (Table S6, entry 2 vs entry 3). This shows the challenge of combining the **Ru-1** promoted-hydrogenation of CO_2 to formate, being favoured at lower temperature, with its conversion to formamide and subsequent hydrogenation to CH_3OH, which instead require more forcing conditions.[72] As the temperature increases, the back reaction, formate dehydrogenation, becomes faster, despite the total applied pressure of 80 bars.[49, 73] Meanwhile, as the amount of formamide accumulates, so does the water by-product, and formamide hydrolysis back to formate might also set in.[74] Water removal by the use of molecular sieves, in order to mitigate formamide hydrolysis and further promote its conversion to CH_3OH, however, was not effective (Table S3, entry 5). CO was detected above 110 °C and steadily increased at higher temperature up to 0.13 mmol at 165 °C (Table S6, entry 8).

Influence of CO_2/H_2 Ratio

Literature data reported the positive influence that a lower relative ratio of the CO_2/H_2 pressure has on mitigating CO production in the hydrogenation of CO_2 to CH_3OH[76] (CO acts as a poison to the catalyst, *vide infra*) while improving CH_3OH yield.[76, 78] To test whether this applies also to our system, experiments were carried out in which the initial CO_2 pressure was lowered while keeping the total pressure of CO_2 and H_2 at 80 bars (Figure 3 and Table S7). Figure 3 clearly shows that by reducing the CO_2 pressure from 30 to −5 bars the amount of CO underwent an almost three-fold cut, from 0.13–0.05 mmol (Table S7, entries 1–4) due to the lower concentration of CO_2 in

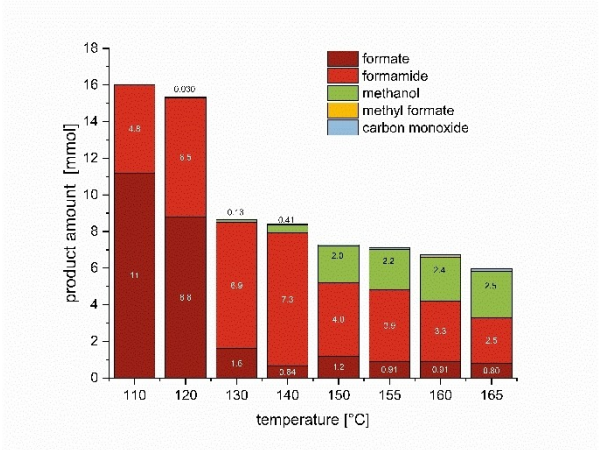

Figure 2. Product distribution as a function of the temperature in the Ru-1 promoted hydrogenation of CO_2. Reaction conditions: TBA·Arg (5.0 mmol), Ru-1 (10 μmol), THF (10 mL), CO_2/H_2 (20/60 bar), 24 h. Numbers represent amounts (mmol) of formate, formamide and methanol, respectively.

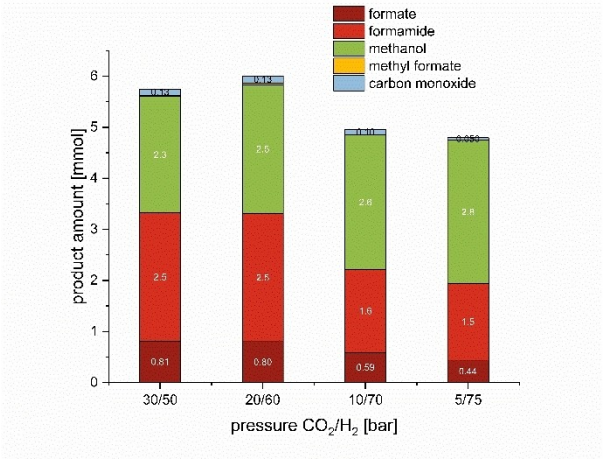

Figure 3. Product distribution as a function of relative CO_2/H_2 pressure in the **Ru-1** promoted hydrogenation of CO_2. Reaction conditions: TBA·Arg (5.0 mmol), **Ru-1** (10 μmol), THF (10 mL), T 165 °C, total pressure 80 bar, 24 h. Numbers represent amounts (mmol) of formate, formamide, methanol and carbon monoxide, respectively.

solution. Moreover, the absolute amount of CH_3OH increased from 2.3 mmol at 30 bars CO_2 (Table S7, Entry 1) to 2.8 mmol at 5 bars CO_2 (Table S7, entry 4), clearly showing the additional positive effect of a higher H_2 pressure on formamide hydrogenation.

Influence of Catalyst Type

Next, other catalysts were applied to assess whether CH_3OH productivity might be improved by varying ligand structure and metal. The tests were done at 150 °C, the temperature at which Ru-MACHO-BH **Ru-1** demonstrated the best trade-off between stability and catalyst turnover number. In fact, experiments carried out at 165 °C, showed that no further formate and CH_3OH were formed after 72 hours (Table S8, entry 13, 0.26 and 2.3 mmol, respectively) compared to those detected after 24 hours (Table S8, entry 13, 0.80 and 2.5 mmol, respectively), clearly indicating catalyst degradation after prolonged heating at this temperature (Figure 4a). Instead, the amount of CH_3OH could be increased to 2.7 mmoles when CO_2 hydrogenation was carried out at 150 °C for 48 hours (Figure 4b and Table S8, entry 8). The tested catalysts are shown in Scheme 2 and the results are collected in Table 2. When the phenyl substituents were replaced by more electron donating *iso*-propyl groups as in **Ru-2** (Table 2, entry 2), a slightly higher amount of formate but a lower one of CH_3OH were obtained. After verifying that **Ru-3**, the chloride analogue of **Ru-1**, is also a competent catalyst for the hydrogenation of CO_2 to CH_3OH (Table 2, entry 3), catalyst **Ru-4**, was tested (Table 2, entry 4), in which the hydrogen at the ligand nitrogen has been replaced by a methyl group.

By comparing entry 3 with entry 4 in Table 2, it is evident that **Ru-4** does indeed promote CO_2 hydrogenation to formate but is much less effective in the subsequent hydrogenolysis of the formamide to CH_3OH.[76] A similar behavior had been observed by Prakash and co-workers in the **Ru-4**-catalysed amine-assisted hydrogenation of CO_2 to CH_3OH. This indicates that ligand-metal cooperativity, with the –NH moiety serving as a hydrogen bond donor for substrate activation towards hydride nucleophilic attack[79] is mandatory for the successful hydrogenation of formamides to CH_3OH via formaldehyde, but not necessary for the hydrogenation of CO_2 to formate.[80] Replacing ruthenium with 1st row-transition metals, either manganese in **Mn-1** (Table 2, entry 5) or iron in **Fe-1** (Table 2, entry 6), noticeably reduced the yield in formate and practically suppressed CH_3OH formation.[82] This confirms previous findings

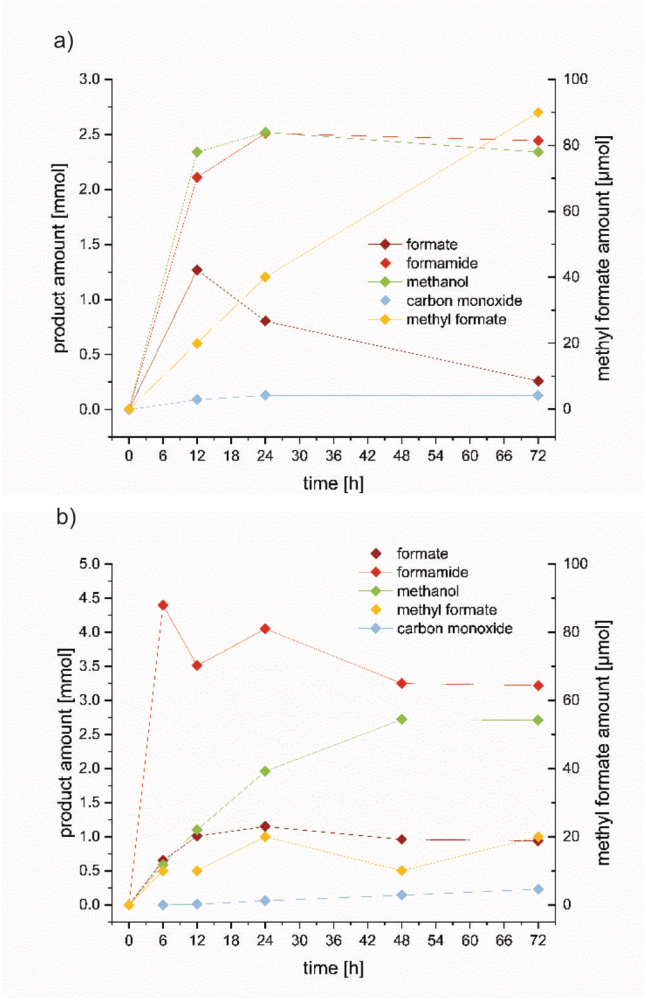

Figure 4. a
Product distribution as a function of reaction time in the **Ru-1** promoted hydrogenation of CO_2 at 165 °C. Reaction conditions: TBA·Arg (5.0 mmol), **Ru-1** (10 µmol), THF (10 mL), CO_2/H_2 (20/60 bar).b
Product distribution as a function of reaction time in the **Ru-1** promoted hydrogenation of CO_2 at 150 °C. Reaction conditions: TBA·Arg (5.0 mmol), **Ru-1** (10 µmol), THF (10 mL), CO_2/H_2 (20/60 bar).

that with catalysts **Mn-1**[83] and **Fe-1**[84] the direct amine-aided hydrogenation of CO_2 to CH_3OH is not possible[27] but requires a one-pot two-step procedure whereby, after hydrogenation of CO_2 to $HCOO^-$, excess CO_2 must be released for the hydrogenation of the ensuing formamide to take place, as CO_2 has an inhibiting effect on the formamide reduction step.[85] This negative influence, although not so pronounced to prevent the

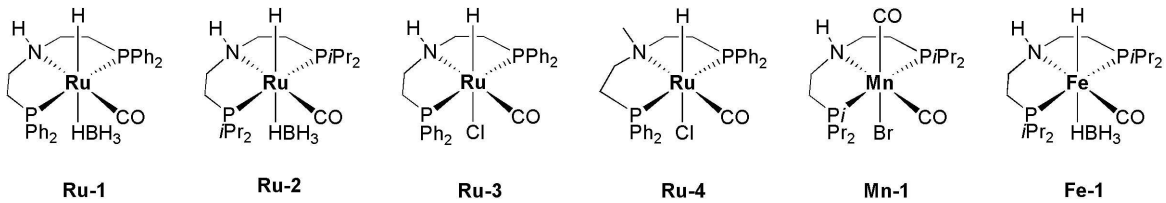

Scheme 2. Catalysts tested in the TBA·Arg-aided hydrogenation of CO_2.

Table 2. TBA·Arg-aided hydrogenation of CO_2 in the presence of different catalyst precursors.

entry	catalyst	Formate[a] [mmol]	Formamide[a] [mmol]	Methanol[b] [mmol]	methyl formate[b] [mmol]	carbon monoxide[c] [mmol]
1	**Ru-1**	1.2	4.0	2.0	0.02	0.06
2	**Ru-2**	1.3	5.4	1.1	0.02	0.007
3	**Ru-3**	0.81	3.0	2.1	0.01	0.07
4	**Ru-4**	0.73	4.2	0.03	n.d.	1.5
5	**Mn-1**	0.41	4.5	0.02	n.d.	n.d.
6	**Fe-1**	0.10	2.9	n.d.	n.d.	0.01

General conditions: TBA·Arg (5.0 mmol), catalyst (10 μmol), THF (10 mL), CO_2/H_2 (20/60 bar), 165 °C, 24 h. [a] Determined by ^{1}H NMR with DMF (200 μL, 2.6 mmol) as internal standard. [b] Determined by GC with DMF (200 μL, 2.6 mmol) as internal standard. [c] Determined by gas GC. Experiments in entries 1–3 were at least performed twice, and average values are shown. Standard deviations of main product amounts (formate, formamide, methanol) are 1–15% of the average (except methyl formate and carbon monoxide amounts < 0.10 mmol).

one-pot one-step procedure, is observed also with **Ru-1**, as shown previously (Figure 3). Only a slight improvement in CH_3OH productivity was observed when, compared to the one pot one step procedure at 165 °C (Table S9, entry 1, 2.3 mmol), after the first step and release of excess CO_2, further formamide reduction was made possible by pressurizing the autoclave again but only with hydrogen at 60 bars (Table S9, entry 2, 2.6 mmol). In this respect, much more effective was the addition of a second batch of **Ru-1** for further hydrogenation (Table S9, entry 3, CH_3OH 3.0 mmol), thus confirming catalyst thermal degradation after prolonged heating as the main reason for unconverted formamide.

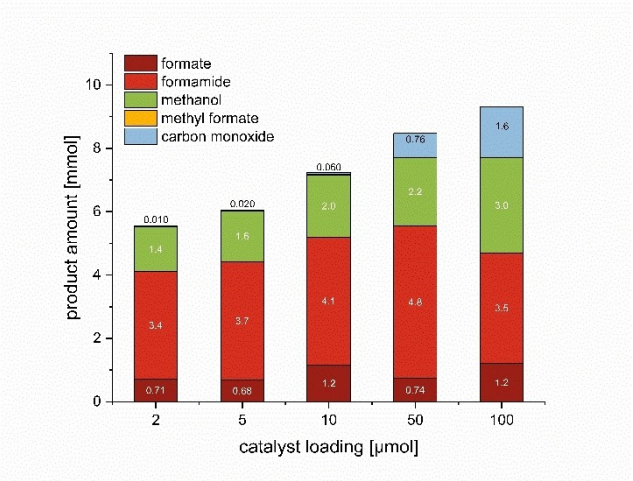

Figure 5. Product distribution as a function of catalyst loading in the **Ru-1** promoted hydrogenation of CO_2 at 150 °C. Reaction conditions: TBA·Arg (5.0 mmol), THF (10 mL), CO_2/H_2 (20/60 bar), 24 h. Numbers represent amounts (mmol) of formate, formamide, methanol and carbon monoxide, respectively.

Influence of Catalyst Amount

As to the influence of catalyst loading, increasing the catalyst amount from 5–100 μmol resulted in almost doubling the amount of CH_3OH (1.6 vs 3.0 mmol; Figure 5 and Table S11, entries 2–5). Furthermore, by extending the reaction time to 48 hours (Table S11, entry 6) another 20% CH_3OH yield improvement was scored. While the lowest methanol amount (1.4 mmol) was obtained applying 2 μmol of catalyst, this represents the highest achieved turnover number (TON: 700, Table S11, entry 1). Notably, in all experiments, variable amounts of CO were detected.

When hydrogenation of CO_2 was carried out using Arg·TBA in THF with **Ru-1** at a pressure of CO_2/H_2 20/60 bars, the amount of detected CO rose at higher temperatures (Table S6) and longer reaction times (Table S8). The amount of CO was also related to the relative pressure of CO_2, increasing at higher CO_2/H_2 ratio, parallel to a higher yield in $HCOO^-$ and lower yield in CH_3OH (Table S7). No CO was detected when equimolar amounts of Arg·TBA and HCOOK were subjected to 60 bars H_2 at 165 °C in the presence of **Ru-1** (Table S10, entry 2), which provides evidence against formate as the source of CO. A strong positive dependency was observed on catalyst concentration (Table S11): when hydrogenation was carried out in 10 mL THF at CO_2/H_2 20/60 bars, 1500000 °C, for 24 hours, CO increased from 0.01 mmol (Table S11, entry 1)–1.6 mmol (Table S11, entry 5) when the amount of **Ru-1** was varied from 2 μmol–100 μmol. Elongating the reaction time to 48 hours the amount of CO almost doubled, reaching 2.7 mmoles (Table S11, entry 6).

While no in-depth investigation was made to disclose the origin of CO, the temperatures (120–165 °C) and H_2/CO_2 total pressure (80 bars) applied in this system are compatible with the reverse water gas shift reaction being one possible source of the detected CO.[86] Besides, CO might arise from decarbonylation of formaldehyde, the first product of formamide hydrogenation *en route* to CH_3OH. Interestingly, **Ru-4**, with a methyl at the ligand nitrogen, also afforded a high amount of CO, 1.5 mmol, but almost no CH_3OH, when compared to catalyst **Ru-1**, 0.06 mmol CO, 2.0 mmol CH_3OH (Table 2, entries 4 and 1, respectively). Excess CO represents a poison to the catalyst, due to the formation of a ruthenium dicarbonyl species, as established by Prakash in a detailed investigation into the ruthenium-pincer-catalyzed amine-assisted homogeneous hy-

drogenation of CO_2 to methanol.[89] Indeed when hydrogenation of CO_2 was carried out using RuMACHO·BH **Ru-1** in the presence of CO from the very beginning, a lower yield in CH_3OH was obtained as to the same reaction without exogenous CO (Table S12, entry 2 vs entry 1, 2.4 vs 3.0 mmol). The absolute amounts of formate and formamide instead were substantially unaffected, thus confirming Prakash's findings that the biscarbonyl complex is able to catalyze the hydrogenation of CO_2 to formate salts but is unable to catalyze the formamide hydrogenation to methanol and amine.[89] The dicarbonyl species can be reverted back to the active ruthenium dihydride at high hydrogen pressure. The lower efficiency of **Ru-2** compared to **Ru-1** as to CH_3OH yield (Table 2, entry 2 vs entry 1) can therefore be ascribed to the higher sensitivity of the latter to CO: in **Ru-2**, the Ru–CO bond is stronger, due to the higher electron density at the metal, which renders CO displacement by hydrogen more demanding.[89] Finally, the effect of dilution and absorbent amount on methanol productivity were analyzed. By increasing the amount of THF, from 10–20 up to 30 ml (Table S13), the amount of CH_3OH slightly increased from 3.0–3.2 up to 3.8 mmol. The most striking influence was on CO formation which was more than halved by dilution, going from 1.6 (Table S13, entry 1) to 0.72 mmoles at the highest dilution (Table S13, entry 3). This result is in line with what observed at higher catalyst concentration (Table S11). Doubling the amount of TBA·Arg from 5 (Table S14, entry 1) to 10 mmol (Table S14, entry 2), in 10 mL THF under otherwise identical conditions, more than doubled the amount of formate and formamide (1.2 vs 2.1 mmol and 3.5 vs 9.8 mmol, respectively) while this had only limited effect on CH_3OH, the amount of which only went from 3.0–3.8 mmol. This result demonstrates that TBA·Arg is a good candidate for CO_2 capture and activation towards **Ru-1** promoted hydrogenation to formate and its subsequent condensation to formamide, yet further reduction of the latter to CH_3OH is quite demanding.

Based on the information gathered through screening of ionic liquids, catalyst precursors and reaction parameters, an experiment combining all potentially favorable conditions was performed enabling an almost threefold increase of methanol yield to 5.8 mmol (Figures 5–6 and Table S15). As to the ionic liquid, the combination of the TBA cation and the L-arginine anion provided the best reaction system among those tested. Although the two basic amino acid L-arginine and L-lysine may be both combined with the TBA cation, to afford ionic liquids which are equally effective in the capture of CO_2 and its further **Ru-1**-catalyzed hydrogenation to formate (Table 1, entry 1 vs entry 2), the L-arginine anion if far more "helpful" in the subsequent hydrogenation to CH_3OH. The main difference between the two is the presence of the guanidino group in L-arginine.

TBA·Arg. is synthetized from an aqueous solution of NBu_4·OH and L-arginine in its zwitterionic form.[90] Despite prolonged heating under high vacuum, the resulting ionic liquid is invariably contaminated with "confined" water.[91] As a result, the side-chain guanidino group, with its very high $pK_{a3} =$ 13.8,[93] is protonated and prefers to form a bound hydroxo complex, even in the presence of high hydroxide ion concentration (with or without the additional presence of water).[94] This also explains why the protonated guanidino group, unlike the α-NH_2 of the arginine anion, is not formylated. Yet the amount of methanol obtained with TBA·GB is comparable to that obtained with TBA·Arg (Table 1, entry 1 vs entry 14). In this case CH_3OH likely arises from **Ru-1** catalyzed ester hydrogenation. Both *n*-BuOH, arising from base promoted degradation of the TBA cation, and *n*-BuOOCH, have been detected in the THF post-reaction solution when TBA·GB was used (Figure S13–S14). However, the TBA cation degradation is observed even with TBA·Lys. Yet the amount of CH_3OH detected is inferior to that provided by CO_2 hydrogenation in the presence of TBA·GB under otherwise identical conditions (Table S16). Therefore, we conclude that the guanidinio group is crucial for CH_3OH formation.

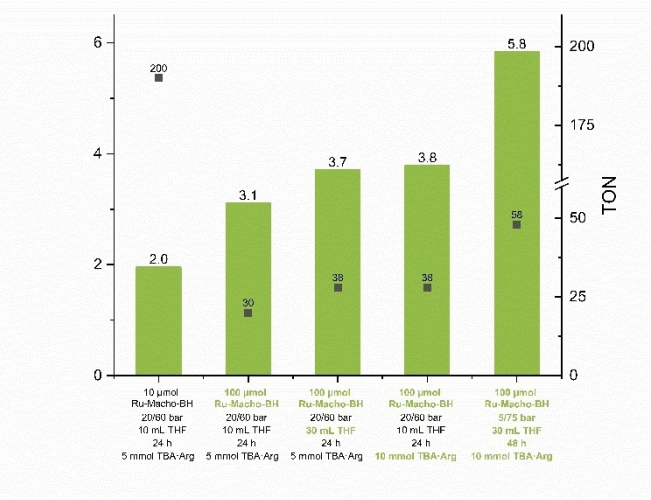

Figure 6. TBA·Arg-aided hydrogenation of CO_2 promoted by Ru-MACHO-BH **Ru-1** under stepwise optimized conditions. General conditions: Ionic liquid TBA·Arg, solvent, catalyst, pressure CO_2/H_2 (bar/bar), 150 °C.

It is known that unsubstituted or mono-substituted guanidinium cations are strong H-bond donors and by establishing hydrogen bonding interactions with proper substrates they can accelerate and control organic reactions.[95] In the present case, interaction of the arginine moiety with either formamide or formate esters may enhance their electrophilic character and thus favor their reduction, contributing to the superior performance of TBA· Arg. However, it might also contribute to CO_2 activation in the first place: L-arginine is the most common amino acid in CO_2 binding pockets of enzymes.[95, 97] The available solid state structures of CO_2 binding proteins show a common motif in which the protonated side chain of a basic amino acid residue, either arginine or lysine, is hydrogen bonded to one oxygen atom of CO_2.[98] As a result, CO_2 is further polarized making the central carbon more electrophilic and thus more reactive to nucleophilic attack. Unfortunately, the productivity in CH_3OH could not be improved by recycling experiments because, under the applied conditions, the TBA cation underwent base degradation to tributyl amine, butene and butanol (Figure S7). The extent of degradation was mainly affected by the temperature (Figure S17) but blank experiments

showed that also the **Ru-1** hydride, as nucleophile, can probably attack the TBA cation, as degradation was less in the absence of hydrogen (Table S2, entry 3 vs entry 4).

Yet, we have demonstrated that TBA·Arg can effectively chemisorb CO_2 and "activate" it towards its catalytic hydrogenation to formate and CH_3OH, without the need for extra base or additives. This is due to the presence of an amino group capable of fixing CO_2, an integrated strong base for catalyst turnover and a hydrogen bond donor for substrate activation. Direct CO_2 capture from air was also possible, although limited to a captured CO_2/TBA·Arg ratio of 0.35, (to be compared with 1.09 in water[57]) due to the poor solubility of TBA·Arg in 1,4-dioxane at room temperature (S8, Figure S19). The captured CO_2 could be hydrogenated under the optimized conditions with 94% conversion and 80% selectivity in CH_3OH (Table S17).

Alternative processes can be envisaged where these features can be advantageously exploited to transform CO_2 in added value products, which however do not require forcing conditions which induce cation degradation. Investigations in this direction are currently underway in our laboratory.

Acknowledgements

We gratefully acknowledge the support from the Federal Ministry of Education and Research (BMBF) and the State of Mecklenburg-Vorpommern. Financial support by the Leibniz Association (Project SUPREME) is also acknowledged. The authors thank the analytical staff of the Leibniz Institute for Catalysis, Rostock, for their excellent service. Open Access funding enabled and organized by Projekt DEAL.

Conflict of Interests

The authors declare no conflict of interest.

Data Availability Statement

The data that support the findings of this study are available in the supplementary material of this article.

Keywords: CO_2 capture · Ionic liquid · Amino acid · Formate · Catalyst · Methanol

[1] *NOAA climate. gov*, United States **2023**, see https://www.climate.gov/news-features/understanding-climate/climate-change-atmospheric-carbon-dioxide (accessed on Mai 13th, **2024**).
[2] *United Nations Climate Change.* Germany **2024**, see https://unfccc.int/process-and-meetings/the-paris-agreement (accessed on Mai 13th, **2024**).
[3] K. Sanderson, *Nature* **2023**, *624*, 484–485.
[4] J. G. Vitillo, M. D. Eisaman, E. S. Aradottir, F. Passarini, T. Wang, S. W. Sheehan, *IScience* **2022**, *25*, 104237.
[5] A. Kätelhön, R. Meys, S. Deutz, S. Suh, A. Bardow, *PNAS* **2019**, *116*, 11187–11194
[6] N. MacDowell, N. Florin, A. Buchard, J. Hallett, A. Galindo, G. Jackson, C. S. Adjiman, C. K. Williams, N. Shah, P. Fennell, *Energy Environ. Sci.* **2010**, *3*, 1645–1669.
[7] *Chemistryviews*. Germany **2024**. See https://www.chemistryviews.org/largest-co2-removal-plant/ (accessed on June 3rd, **2024**).
[8] J. Artz, T. E. Müller, K. Thenert, J. Kleinekorte, R. Meys, A. Sternberg, A. Bardow, W. Leitner, *Chem. Rev.* **2018**, *118*, 434–504.
[9] M. C. Freyman, Z. Huang, D. Ravikumar, E. B. Duoss, Y. Li, S. E. Baker, S. H. Pang, J. A. Schaidle, *Joule* **2023**, *7*, 631–651.
[10] M. Zanatta, *ACS Mater. Au* **2023**, *3*, 576–583.
[11] R. E. Siegel, S. Pattanayak, L. A. Berben, *ACS Catal.* **2022**, *13*, 766–784.
[12] S.-T. Bai, G. De Smet, Y. Liao, R. Sun, C. Zhou, M. Beller, B. U. Maes, B. F. Sels, *Chem. Soc. Rev.* **2021**, *50*, 4259–4298.
[13] Y. Xu, L. Wang, Q. Zhou, Y. Li, L. Liu, W. Nie, R. Xu, J. Zhang, Z. Cheng, H. Wang, *Coord. Chem. Rev.* **2024**, *508*, 215775.
[14] A. Álvarez, A. Bansode, A. Urakawa, A. V. Bavykina, T. A. Wezendonk, M. Makkee, J. Gascon, F. Kapteijn, *Chem. Rev.* **2017**, *117*, 9804–9838.
[15] R. Sen, A. Goeppert, G. S. Prakash, *Angew. Chem. Int. Ed.* **2022**, *61*, e202207278.
[16] N. Onishi, Y. Himeda, *Chem. Catal.* **2022**, *2*, 242–252.
[17] G. A. Olah, *Angew. Chem. Int. Ed.* **2013**, *52*, 104–107.
[18] G. A.Olah, A.Geoppert, G. S.Prakash, Beyond Oil and Gas: *the Methanol Economy*, 3rd ed: *Wiley-VCH*: Weinheim, Germany, **2018**. ISBN 978-3-527-80567-9.
[19] S. S. Tabibian, M. Sharifzadeh, *Renewable Sustainable Energy Rev.* **2023**, *179*, 113281.
[20] A publication of the International Renewable Energy Agency, www.irena.org. IRENA and Methanol Institute 2021, Innovation Outlook: Renewable Methanol, International Renewable Energy Agency, Abu Dhabi. ISBN: 978–92-9260-320-5.
[21] Methanol Institue. United States 2024. See https://ww.methanol.org/applications/ (accessed May 2024) .
[22] B. Dutcher, M. Fan, A. G. Russell, *ACS Appl. Mater. Interfaces* **2015**, *7*, 2137–2148.
[23] N. M. Rezayee, C. A. Huff, M. S. Sanford, *J. Am. Chem. Soc.* **2015**, *137*, 1028–1031.
[24] S. Kar, A. Goeppert, G. S. Prakash, *Acc. Chem. Res.* **2019**, *52*, 2892–2903.
[25] R. Sen, C. J. Koch, A. Goeppert, G. S. Prakash, *ChemSusChem* **2020**, *13*, 6318–6322.
[26] R. Sen, A. Goeppert, S. Kar, G. S. Prakash, *J. Am. Chem. Soc.* **2020**, *142*, 4544–4549.
[27] S. Kar, R. Sen, A. Goeppert, G. S. Prakash, *J. Am. Chem. Soc.* **2018**, *140*, 1580–1583.
[28] L. Zhang, M. Pu, M. Lei, *Dalton Trans.* **2021**, *50*, 7348–7355.
[29] Y. Yamazaki, M. Miyaji, O. Ishitani, *J. Am. Chem. Soc.* **2022**, *144*, 6640–6660.
[30] R. Sen, A. Goeppert, G. S. Prakash, *Aldrichimica Acta* **2020**, *53*, 39–56.
[31] C. J. Nielsen, H. Herrmann, C. Weller, *Chem. Soc. Rev.* **2012**, *41*, 6684–6704.
[32] R. Ramezani, S. Mazinani, R. Di Felice, *Rev. Chem. Eng.* **2022**, *38*, 273–299.
[33] V. Sang Sefidi, P. Luis, *Ind. Eng. Chem. Res.* **2019**, *58*, 20181–20194.
[34] D. Wei, H. Junge, M. Beller, *Chem. Sci.* **2021**, *12*, 6020–6024.
[35] D. Wei, R. Sang, P. Sponholz, H. Junge, M. Beller, *Nat. Energy* **2022**, *7*, 438–447.
[36] N. Guntermann, G. Franciò, W. Leitner, *Green Chem.* **2022**, *24*, 8069–8075.
[37] S. Shen, Y. Yang, Y. Bian, Y. Zhao, *Environ. Sci. Technol.* **2016**, *50*, 2054–2063.
[38] C.-Y. Cheng, H. Shen, N.-N. Shen, C. Castro, V. Dubovoy, D. Wu, R. Subramanyan, X.-Y. Huang, C. E. Pitsch, X. Wang, *Ind. Eng. Chem. Res.* **2021**, *60*, 17745–17749.
[39] S. Shen, Y.-n Yang, *Energy Fuels* **2016**, *30*, 6585–6596.
[40] S. Shen, X. Feng, R. Zhao, U. K. Ghosh, A. Chen, *Chem. Eng. J.* **2013**, *222*, 478–487.
[41] S. Zeng, X. Zhang, L. Bai, X. Zhang, H. Wang, J. Wang, D. Bao, M. Li, X. Liu, S. Zhang, *Chem. Rev.* **2017**, *117*, 9625–9673.
[42] G. Cui, J. Wang, S. Zhang, *Chem. Soc. Rev.* **2016**, *45*, 4307–4339.
[43] T. Sasaki, *Curr. Opin. Green Sustainable Chem.* **2022**, *36*, 100633.
[44] M. I. Qadir, J. Dupont, *Angew. Chem. Int. Ed.* **2023**, *62*, e202301497.
[45] T. Schaub, R. A. Paciello, *Angew. Chem. Int. Ed.* **2011**, *32*, 7278–7282.
[46] A. Weilhard, S. P. Argent, V. Sans, *Nat. Commun.* **2021**, *12*, 231.
[47] A. Weilhard, M. I. Qadir, V. Sans, J. Dupont, *ACS Catal.* **2018**, *8*, 1628–1634.

[48] A. Weilhard, K. Salzmann, M. Navarro, J. Dupont, M. Albrecht, V. Sans, *J. Catal.* **2020**, *385*, 1–9.
[49] L. Piccirilli, B. Rabell, R. Padilla, A. Riisager, S. Das, M. Nielsen, *J. Am. Chem. Soc.* **2023**, *145*, 5655–5663.
[50] G. Gurau, H. Rodríguez, S. P. Kelley, P. Janiczek, R. S. Kalb, R. D. Rogers, *Angew. Chem. Int. Ed* **2011**, *50*, 12024.
[51] W. Ma, J. Hu, L. Zhou, Y. Wu, J. Geng, X. Hu, *Green Chem.* **2022**, *24*, 6727–6732.
[52] C. J. Koch, A. Goeppert, G. Surya Prakash, *ChemSusChem* **2024**, *17*, e202301789.
[53] S. Saravanamurugan, A. J. Kunov-Kruse, R. Fehrmann, A. Riisager, *ChemSusChem* **2014**, *7*, 897–902.
[54] E. A. Recker, M. Green, M. Soltani, D. H. Paull, G. J. McManus, J. H. Davis Jr, A. Mirjafari, *ACS Sustainable Chem. Eng.* **2022**, *10*, 11885–11890.
[55] H. Ohno, K. Fukumoto, *Acc. Chem. Res.* **2007**, *40*, 1122–1129.
[56] S. Kirchhecker, D. Esposito, *Curr. Opin. Green Sustainable Chem.* **2016**, *2*, 28–33.
[57] A. Moazezbarabadi, D. Wei, H. Junge, M. Beller, *ChemSusChem* **2022**, *15*, e202201502.
[58] Z. Song, Y. Liang, M. Fan, F. Zhou, W. Liu, *RSC Adv.* **2014**, *4*, 19396–19402.
[59] W. Fang, Y. Zhang, Z. Yang, Z. Zhang, F. Xu, W. Wang, H. He, Y. Diao, Y. Zhang, Y. Luo, *Appl. Catal., A* **2021**, *617*, 118111.
[60] M. Guncheva, P. Ossowicz, E. Janus, S. Todinova, D. Yancheva, *J. Mol. Liq.* **2019**, *283*, 257–262.
[61] Y. S. Sistla, A. Khanna, *Chem. Eng. J.* **2015**, *273*, 268–276.
[62] X.-D. Lang, S. Zhang, Q.-W. Song, L.-N. He, *RSC Adv.* **2015**, *5*, 15668–15673.
[63] J. Kothandaraman, D. J. Heldebrant, J. S. Lopez, R. A. Dagle, *Front. Energy Res.* **2023**, *11*, 1158499.
[64] J. R. Cabrero-Antonino, R. Adam, V. Papa, M. Beller, *Nat. Commun.* **2020**, *11*, 3893.
[65] O. Ogata, W. Kuriyama, *J. Synth. Org. Chem. Jpn.* **2023**, *81*, 1040–1049.
[66] Y. Wang, J. Zhang, J. Liu, C. Zhang, Z. Zhang, J. Xu, S. Xu, F. Wang, F. Wang, *ChemSusChem* **2015**, *8*, 2066–2072.
[67] B. Xu, M. I. Jacobs, O. Kostko, M. Ahmed, *ChemPhysChem* **2017**, *18*, 1503–1506.
[68] M. Marino, K. Kreuer, *ChemSusChem* **2015**, *8*, 513–523.
[69] D. R. Dekel, S. Willdorf, U. Ash, M. Amar, S. Pusara, S. Dhara, S. Srebnik, C. E. Diesendruck, *J. Power Sources* **2018**, *375*, 351–360.
[70] E. S. Wiedner, J. C. Linehan, *Chem. Eur. J.* **2018**, *24*, 16964–16971.
[71] A. Kaithal, B. Chatterjee, C. Werlé, W. Leitner, *Angew. Chem. Int. Ed.* **2021**, *60*, 26500–26505.
[72] R. Kuhlmann, M. Nowotny, K. U. Künnemann, A. Behr, A. J. Vorholt, *J. Catal.* **2018**, *361*, 45–50.
[73] S. Patra, B. Maji, H. Kawanami, Y. Himeda, *RSC Sustainability* **2023**, *1*, 1655–1671.
[74] H. Ślebocka-Tilk, A. A. Neverov, R. Brown, *J. Am. Chem. Soc.* **2003**, *125*, 1851–1858.
[75] J. Blumberger, B. Ensing, M. L. Klein, *Angew. Chem. Int. Ed.* **2006**, *45*, 2893.
[76] J. Kothandaraman, A. Goeppert, M. Czaun, G. A. Olah, G. S. Prakash, *J. Am. Chem. Soc.* **2016**, *138*, 778–781.
[77] A. Bansode, A. Urakawa, *J. Catal.* **2014**, *309*, 66–70.
[78] F. H. Zhang, C. Liu, W. Li, G. L. Tian, J. H. Xie, Q. L. Zhou, *Chin. J. Chem.* **2018**, *36*, 1000–1002.
[79] P. A. Dub, J. C. Gordon, *Nat. Rev. Chem.* **2018**, *2*, 396–408.
[80] P. A. Dub, B. L. Scott, J. C. Gordon, *J. Am. Chem. Soc.* **2017**, *139*, 1245–1260.
[81] A. Agapova, E. Alberico, A. Kammer, H. Junge, M. Beller, *ChemCatChem* **2019**, *11*, 1910–1914.
[82] T. Singh, S. Jalwal, S. Chakraborty, *Asian J. Org. Chem.* **2022**, *11*, e202200330.
[83] S. Kar, A. Goeppert, J. Kothandaraman, G. S. Prakash, *ACS Catal.* **2017**, *7*, 6347–6351.
[84] E. M. Lane, Y. Zhang, N. Hazari, W. H. Bernskoetter, *Organometallics* **2019**, *38*, 3084–3091.
[85] A. Singh, G. Kemper, T. Weyhermüller, N. Kaeffer, W. Leitner, *Chem. Eur. J.* **2024**, *30*, e202303438.
[86] M. Taqui Khan, S. Halligudi, S. Shukla, *J. Mol. Catal.* **1989**, *57*, 47–60.
[87] K. Tsuchiya, J.-D. Huang, K.-i Tominaga, *ACS Catal.* **2013**, *3*, 2865–2868.
[88] D. U. Nielsen, X.-M. Hu, K. Daasbjerg, T. Skrydstrup, *Nat. Catal.* **2018**, *1*, 244–254.
[89] S. Kar, R. Sen, J. Kothandaraman, A. Goeppert, R. Chowdhury, S. B. Munoz, R. Haiges, G. S. Prakash, *J. Am. Chem. Soc.* **2019**, *141*, 3160–3170.
[90] A. R. Carreira, S. N. Rocha, F. A. e Silva, T. E. Sintra, H. Passos, S. P. Ventura, J. A. Coutinho, *Fluid Phase Equilib.* **2021**, *542*, 113091.
[91] M. Zanatta, A.-L. Girard, G. Marin, G. Ebeling, F. P. Dos Santos, C. Valsecchi, H. Stassen, P. R. Livotto, W. Lewis, J. Dupont, *Phys. Chem. Chem. Phys.* **2016**, *18*, 18297–18304.
[92] M. Zanatta, N. M. Simon, J. Dupont, *ChemSusChem* **2020**, *13*, 3101–3109.
[93] C. A. Fitch, G. Platzer, M. Okon, B. Garcia-Moreno, E. L. P. McIntosh, *Protein Sci.* **2015**, *24*, 752–761.
[94] A. T. Banyikwa, S. E. Miller, R. A. Krebs, Y. Xiao, J. M. Carney, M. S. Braiman, *ACS Omega* **2017**, *2*, 7239–7252.
[95] Y. Kobayashi, Y. Takemoto, Bifunctional Guanidine as Hydrogen-Bond-Donating Catalysts, in P. Selig Eds. Guanidine as Reagents and Catalysts I, Topics in Heterocyclic Chemistry, vol. 50, 2015, Springer, Cham. https://doi 10.1007/7081_2015_155.
[96] J. Hu, J. Ma, H. Liu, Q. Qian, C. Xie, B. Han, *Green Chem.* **2018**, *20*, 2990–2994.
[97] T. R. Cundari, A. K. Wilson, M. L. Drummond, H. E. Gonzalez, K. R. Jorgensen, S. Payne, J. Braunfeld, M. De Jesus, V. M. Johnson, *J. Chem. Inf. Model.* **2009**, *49*, 2111–2115.
[98] M. L. Drummond, A. K. Wilson, T. R. Cundari, *J. Phys. Chem. B* **2012**, *116*, 11578–11593.

Manuscript received: August 16, 2024
Revised manuscript received: October 22, 2024
Accepted manuscript online: November 9, 2024
Version of record online: ■■, ■■